Dependence of Edge Stability on Plasma Shape and Local Pressure Gradients in the DIII–D and JT-60U Tokamaks* **EX**

L.L. Lao, K.H. Burrell, M.S. Chu, J.R. Ferron, G.L. Jackson, T.H. Osborne, P.B. Snyder, E.J. Strait, A.D. Turnbull, V.S. Chan, T.S. Taylor
email: lao@fusion.gat.com
General Atomics, P.O. Box 85608, San Diego, California 92186-5608, USA

Y. Kamada, T. Oikawa, S. Takeji, T. Takizuka, T. Hatae, A. Isayama, T.Fukuda, and K. Tsuchiya
Naka Fusion Research Establishment, JAERI, Naka-machi, Naka-gun, Ibaraki-ken, Japan

L.R. Baylor, M. Murakami, M.R. Wade
Oak Ridge National Laboratory, Oak Ridge, Tennessee, 37381 USA

M. A. Makowski
Lawrence Livermore National Laboratory, Livermore 94550, California USA

M. Chance, J. Manickam, M. Okabayashi
Princeton Plasma Physics Laboratory, Princeton, New Jersey 08543, USA

The improved confinement in the edge region of H–mode discharges often leads to instabilities driven by the large pedestal pressure gradient P′ and bootstrap current density J_{BS}. The discharge performance is sensitive to the magnitude of the pedestal pressure, which is limited by these edge localized modes (ELMs). Discharge shaping provides a powerful tool for varying the stability properties of the plasma edge. DIII–D discharges have high elongation $\kappa \geq 1.8$, low to high triangularity (δ) and squareness (ξ), whereas JT-60U discharges have moderate $\kappa \sim 1.4$ and low to moderate δ. The stronger plasma shaping allows the edge region of DIII–D giant ELM discharges to have second ideal ballooning stability access and larger edge P′ than JT-60U discharges, which are bound by the first ballooning stability limit. Comparison of results between these two devices can clarify the effects of plasma shape and pressure pedestal on ELMs, and whether intermediate toroidal mode number (*n*) modes are responsible for giant ELMs in both devices but are masked by unstable high *n* ballooning modes in JT-60U.

Recent DIII–D results support an ideal stability based working model [1] of ELMs as low to intermediate *n* MHD modes. As shown schematically in Fig. 1(a), the most unstable mode

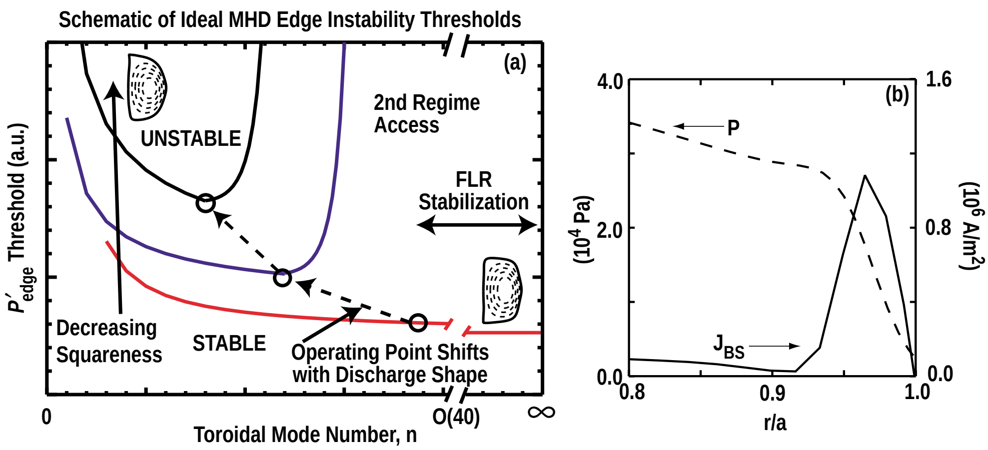

Fig. 1. (a) A schematic drawing of the stability boundaries in the H–mode pedestal region for 3 different discharge shapes with moderate to high squareness. The most unstable mode number is found at the minimum of the P′ threshold curve. (b) Edge P and bootstrap current density for a DIII–D moderate squareness discharge.

*Work supported by U.S. Department of Energy under Contracts DE-AC03-99ER54463, DE-AC05-96OR22464, W-7405-ENG-48, and DE-AC02-76CH03073.

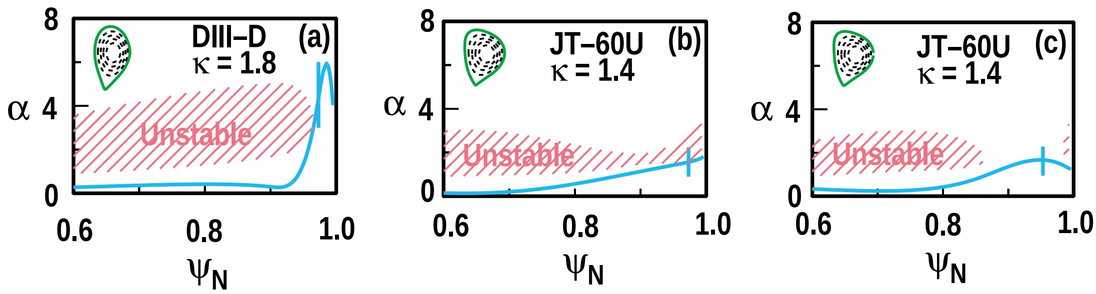

Fig. 2. Comparison of ballooning stability boundary for (a) a DIII–D discharge, (b) a JT-60U discharge, both have giant ELMs and q_{95} ~ 3.4, and (c) a JT-60U grassy ELM discharge with q_{95} ~ 6.0.

number is determined by second regime access for high mode numbers, as well as by discharge shape. The ELM amplitudes are related to the radial width of the unstable modes which depends on the pressure pedestal and J_{BS}. In DIII–D H–mode discharges second ballooning stability access to high *n* modes is found to play an important role in the edge instabilities. The combination of proper discharge shape and sufficient J_{BS} [Fig. 1(b)] allows second ballooning stability access in the pedestal region [Fig. 2(a)]. This access allows the edge P′ to increase to values well above the first ballooning stability limit until a lower *n* coupled kink/ballooning mode is destabilized. In this case large amplitude ELMs are expected due to the large edge P′ and J_{BS}, as typically observed in DIII–D discharges with moderate squareness ξ. Predictions from this model are consistent with the low amplitude ELMs observed in high ξ discharges without second regime access (Fig. 1), and the observed increase of pedestal P′ with δ. The model is also consistent with the observed suppression or modification of ELMs by krypton gas and deuterium pellet injection to modify P′. Quasi-stationary H–mode discharges with saturated MHD modes rather than ELM cycles have also been recently produced in DIII–D with counter-beam injection and cryo-pumping. Comparison of these new observations to predictions from the working ELM model is underway.

Recent JT-60U studies focus on the effects of triangularity δ and edge safety factor q_{95} on the ELM character. Large amplitude, low frequency ELMs (~ 100 Hz) are found to disappear and small, high frequency "grassy" ELMs (~ 500–1000 Hz) to appear at sufficiently large δ $\gtrsim$ 0.45, $q_{95} \gtrsim 5$, and β_P [2]. At intermediate δ and lower q_{95} discharges are observed to consist of mixtures of giant and grassy ELMs. The pedestal P′ in grassy ELM discharges is as high as that in giant ELM discharges. The giant ELM frequency increases almost linearly with the net heating power, whereas the grassy ELM discharges show no clear dependence. Ballooning stability analysis using accurately reconstructed equilibria based on kinetic profiles and MSE measurements shows that the edge region of the grassy ELM discharges has second stability access, whereas the edge region of the giant ELM discharges is bound by the first stability limit [Figs. 2(b), 2(c)]. This is in contrast to the DIII–D results and may be due to the weaker finite *n* correction effects in JT-60U discharges that have lower κ ~ 1.4 (Fig. 2). As shown in Figs. 2(a), 2(b), and 2(c), DIII–D discharges typically have larger edge P′ than JT-60U discharges, consistent with the difference in calculated ballooning mode limits. Detailed low and intermediate *n* stability analysis is underway to compare these JT-60U results against predictions from the DIII–D working ELM model.

[1] J.R. Ferron, *et al.*, "Modification of H–Mode Pedestal Instabilities in the DIII–D Tokamak," submitted to Phys. Plasmas.

[2] Y. Kamada, *et al.*, "Disappearance of Giant ELMs and Appearance of Minute Grassy ELMs in JT-60U Discharges," submitted to Plasma Phys. and Control. Fusion.